Insights into Crystalline Preorganization of Gas-Phase Precursors: Densification Mechanisms

Stéphane Olivier, Jean-Marie Ducéré, Cédric Mastail, Georges Landa, Alain Estève,* and Mehdi Djafari Rouhani

Laboratoire d'Analyse et d'Architecture des Systemes, CNRS, University of Toulouse, 7 Avenue du Colonel Roche, 31077 Toulouse Cedex 4, France

Received July 2, 2007. Revised Manuscript Received September 17, 2007

Using density functional theory calculations, we address the structural phase transition from the covalent metallic precursor molecules to their oxide layer structure during the gas-phase deposition process. We observe that the associated increase in the metal coordination number during the gas–solid transition, i.e., the redistribution mechanisms of oxygen atoms around the metal atoms, are identical and barrierless for Sn- or Hf-based precursors. These mechanisms, occurring in the grown oxide layers, are shown to be present at the early stage of gas phase agglomeration reactions, giving rise to unexpected species. The presence of OH hydroxyl groups on the surface/hydroxylated precursors are mainly responsible for this transition. Finally, we discuss the relevance of our calculations within the framework of the metal oxides growth by ALD process.

1. Introduction

Gas-phase deposition is today a well-established technique used in most thin film materials fabrication. A key technological question that arises during the film growth is the necessary phase transition of the interesting materials from their molecular structure in the gas-phase precursors to their solid-state structure in the deposited film. This is particularly true for metallic compounds such as oxides, where the metal has a covalent bonding structure with a small coordination number in the precursor, whereas the metal oxides have mainly ionic structures with a large coordination number.

The case of HfO_2 layers, used as high-*k* gate oxides in the future generation of MOS (metal oxide semiconductor) transistors, constitutes a relevant example. One of the methods used to grow this kind of film is atomic layer deposition (ALD). In the ALD process, a weakly reactive but moisture sensitive precursor and water are sequentially injected in a vessel, with a purge of the unreacted species preceding the next injection, and then deposited on a initially hydroxilated surface. During ALD of HfO_2 on SiO_2 substrates, it has been experimentally observed that more than 10 cycles are needed to obtain the complete coverage of the substrate surface, despite the basic principle of ALD, which suggests that a complete layer should be obtained after each single cycle. Moreover, the density of the deposited oxide near the substrate surface is much lower than that in the bulk oxide, but increases with increasing film thickness. The origin of this mechanism, usually referred to as densification,[1–8] lies in the above structural phase transition.

Another example is the case of SnO_2 used in the manufacturing of gas sensors, where the fabrication faces similar problems. The Hf element is normally tetracoordinated in usual precursor molecules ($HfCl_4$, TEMAH, . . .), but its coordination can increase to up to eight in HfO_2 in its fluorite structure. Similarly, SnO_2 films show rutile structure. The coordination number of Sn increases from four in the precursor molecule to six in the oxide.

It is worth noting that although an abundant amount of literature is dedicated to precursor/surface physicochemistry, the detailed understanding of the densification mechanisms remains elusive.[9] An insight into basic chemical reaction pathways would certainly help to improve and optimize the deposition process.

The purpose of the present paper is to investigate the atomistic pathways that allow us to achieve the above structural phase transition, in order to allow the design of more efficient technological processes. At the same time, we will examine to what extent this mechanism could be considered as generic and generalized to various metals. The search for reaction pathways will be performed within the Born–Oppenheimer approximation, where the system remains in its fundamental electronic state throughout the reaction. This is in agreement with the experimental conditions where the transition is caused by thermally excited

* Corresponding author. E-mail: aesteve@laas.fr.

(1) Wilk, G. D.; Wallace, R. M.; Anthony, J. M. J. *Appl. Phys.* **2001**, *89*, 5243.
(2) Widjaja, Y.; Musgrave, C. B. *Appl. Phys. Lett.* **2002**, *80*, 3304.
(3) Widjaja, Y.; Musgrave, C. B. *Appl. Phys. Lett.* **2002**, *81*, 304.
(4) Widjaja, Y.; Musgrave, C. B. *J. Chem. Phys.* **2002**, *117*, 1931.
(5) Jeloaica, L.; Dkhissi, A.; Mazaleyrat, G.; Estève, A.; Djafari Rouhani, M. *Comput. Mater. Sci.* **2005**, 33.
(6) Jeloaica, L.; Estève, A.; Djafari Rouhani, M.; Esteve, D. *Appl. Phys. Lett.* **2003**, *82*, 263.
(7) Esteve, A.; Djafari Rouhani, M.; Jeloaica, L.; Estève, D. *Comput. Mater. Sci.* **2003**, *27*, 75.
(8) Mazaleyrat, G.; Jeloaica, L.; Estève, A.; Djafari Rouhani, M. *Comp. Mat. Sci.* **2005**, *33*, 74.
(9) Albernathy, C. R.; Gusev, E. P.; Schlom, D.; Stemmer, S. *MRS Symposium Proceedings: Fundamentals of Novel Oxide/Semiconductor Interfaces*; Estève, A., Jeloaica, L., Mazaleyrat, G., Dkhissi, A., Djafari Rouhani, M., Ali Messaoud, A., Fazouan, N., Eds.; Materials Research Society: Pittsburg, PA, 2004; Vol. 786, p 35.

10.1021/cm071740a CCC: $40.75
Published on Web 01/24/2008

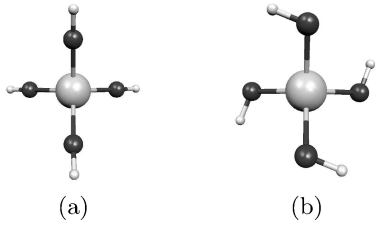

Figure 1. $Hf(OH)_4$ and $Sn(OH)_4$ structures. We notice almost linear Hf−O−H versus significantly bent Sn−O−H enchainments.

Table 1. Geometrical Parameters of $Hf(OH)_4$ and $Sn(OH)_4$

$Hf(OH)_4$	Hf−O	1.948Å
	O−H	0.960Å
	Hf−O−H	178.6°
$Sn(OH)_4$	Sn−O	1.978Å
	O−H	0.975Å
	Sn−O−H	109.7°

atomic vibrations, and not induced optically where electronic excited states are basically observed. Therefore, calculations based on density functional theory (DFT) are carried out in our study. To remain generic, we will consider in the following the simplest cases referring to the above two examples, HfO_2 and SnO_2, under a simple model hydroxylated precursor with water molecules as donors.

Computational details and parameters used in DFT calculations are described in Section 2. We start by optimizing the geometry of the precursor molecules before testing their hydration properties in the presence of water molecules. The formation of dimer molecules is then investigated, and the hydration of dimers is examined. These results are reported and discussed in Section 3, where the relation with the film growth and process optimization is also emphasized. Concluding remarks are presented in Section 4.

2. Computational Details

All the calculations were performed using the Gaussian03 package[10] within the frame of the density functional theory, using the gradient corrected PBE functional.[11] Oxygen and hydrogen were described with the triple-ζ augmented with a polarization function, respectively, *d* and *p*, TZVP basis set.[12] Tin [Ar], $3d^{10}$ core–electrons were replaced with a pseudopotential,[13] whereas remaining valence electrons were treated using a (10s, 9p, 8d, 2f)/[6s, 5p, 3d,2f] basis set.[14] Hafnium [Kr], $4d^{10}$, $4f^{14}$ core was replaced with a pseudopotential,[15] and valence electrons were described with a (8s, 7p, 6d)/[6s, 5p, 3d] basis set.[14] All the stationary points were checked to be real minima thanks to the determination of the vibration frequencies; this allowed us to correct the binding energies of the zero-point vibrational energy. Finally, the basis set superposition error (BSSE) was corrected by the Boys and Bernardi counterpoise scheme.[16]

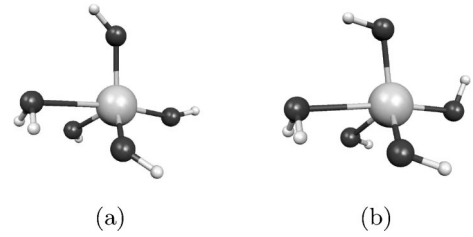

Figure 2. Monohydrated (a) $Hf(OH)_4$ and (b) $Sn(OH)_4$ structures.

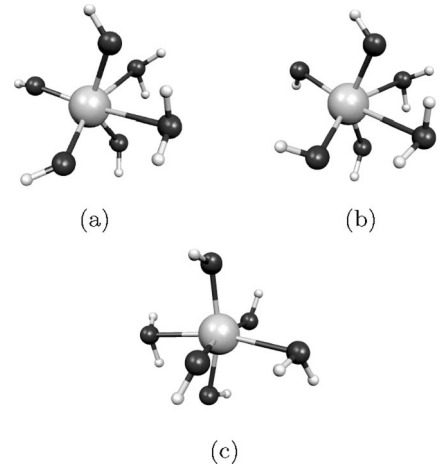

Figure 3. Bihydrated (a) *cis*-$Hf(OH)_4$ and (b) *cis*- and (c) *trans*-$Sn(OH)_4$ structures.

3. Results and Discussion

(A) Hydration of $M(OH)_4$. First, we performed the geometry optimization of the $M(OH)_4$ molecules, M being Hf or Sn (see Figure 1).

Calculated equilibrium distances and angles are represented in Table 1. We can observe that different distances M−O and O−H are almost identical for the two metals. However, the Hf−O bonds are shorter than the Sn−O bonds, which is explained by the higher ionicity of the Hf−O bond.

Second, O−H bonds are slightly shorter in $Hf(OH)_4$ than in $Sn(OH)_4$; that indicates that $Sn(OH)_4$ is a little more acidic because of Sn being a little more electronegative than Hf. On the contrary, we can note that Hf−O−H angles are significantly more open than Sn−O−H angles as Hf−O bonds are more ionic than Sn−O bonds. This configuration already sketches the bulk oxide structure, where $(OH)_3M-O-M(OH)_3$ angles have almost the same values as those in Table 1. Also, the more open Hf−O−Hf angle does not impose a steric restriction, which would prevent a

(10) Frisch, M. J.; Trucks, G. W.; Schlegel, H. B.; Scuseria, G. E.; Robb, M. A.; Cheeseman, J. R.; Montgomery, J. A., Jr.; Vreven, T.; Kudin, K. N.; Burant, J. C.; Millam, J. M.; Iyengar, S. S.; Tomasi, J.; Barone, V.; Mennucci, B.; Cossi, M.; Scalmani, G.; Rega, N.; Petersson, G. A.; Nakatsuji, H.; Hada, M.; Ehara, M.; Toyota, K.; Fukuda, R.; Hasegawa, J.; Ishida, M.; Nakajima, T.; Honda, Y.; Kitao, O.; Nakai, H.; Klene, M.; Li, X.; Knox, J. E.; Hratchian, H. P.; Cross, J. B.; Adamo, C.; Jaramillo, J.; Gomperts, R.; Stratmann, R. E.; Yazyev, O.; Austin, A. J.; Cammi, R.; Pomelli, C.; Ochterski, J. W.; Ayala, P. Y.; Morokuma, K.; Voth, G. A.; Salvador, P.; Dannenberg, J. J.; Zakrzewski, V. G.; Dapprich, S.; Daniels, A. D.; Strain, M. C.; Farkas, O.; Malick, D. K.; Rabuck, A. D.; Raghavachari, K.; Foresman, J. B.; Ortiz, J. V.; Cui, Q.; Baboul, A. G.; Clifford, S.; Cioslowski, J.; Stefanov, B. B.; Liu, G.; Liashenko, A.; Piskorz, P.; Komaromi, I.; Martin, R. L.; Fox, D. J.; Keith, T.; Al-Laham, M. A.; Peng, C. Y.; Nanayakkara, A.; Challacombe, M.; Gill, P. M. W.; Johnson, B.; Chen, W.; Wong, M. W.; Gonzalez C.; Pople, J. A. *Gaussian 03, Revision B.05*; Gaussian Inc.: Pittsburgh, PA, 2003.
(11) Perdew, J. P.; Burke, K.; Ernzerhof, M. *Phys. Rev. Lett.* **1996**, *77*, 3865.
(12) SchÃ-fer, A.; Huber, C.; Ahlrichs, R. J. *Chem. Phys.* **1994**, *100*, 5829.
(13) Metz, B.; Stoll, H.; Dolg, M. J. *Chem. Phys.* **2000**, *113*, 2563.
(14) Weigend, F.; Ahlrichs, R. *Phys. Chem. Chem. Phys.* **2005**, *7*, 3297.
(15) Andrae, D.; Haeussermann, U.; Dolg, M.; Stoll, H.; Preuss, H. *Theor. Chim. Acta* **1990**, *77*, 123.
(16) Boys, S. F.; Bernardi, F. *Mol. Phys.* **1970**, *19*, 553.

Table 2. First and Second $M(OH)_4$ Hydration Energies[a]

complex	$\Delta E_{2\ H_2O}$ (kJ/mol)	ΔE_{H2O}
$Hf(OH)_4(H_2O)$ (Figure 2a)		−32
$Sn(OH)_4(H_2O)$ (Figure 2b)		−41
cis-$Hf(OH)_4(H_2O)_2$ (Figure 3a)	−58	−26
cis-$Sn(OH)_4(H_2O)_2$ (Figure 3b)	−52	−11
trans-$Sn(OH)_4(H_2O)_2$ (Figure 2 c)	−35	+6

[a] For the first hydratation, the energies correspond to the bonding of one water molecule. For the second hydratation, the first column corresponds to the bonding of the two water molecules and the second column to the bonding of the second water molecule on the monohydrated $M(OH)_4$.

huge increase in the coordination number. We are going to investigate this point by hydrating $M(OH)_4$ with water molecules.

We then hydrated $M(OH)_4$. We have compiled in Table 2 the first and second hydration energies for $Hf(OH)_4$ and $Sn(OH)_4$.

We can note that binding the first water molecule (see Figure 2) to Sn is more favorable than binding to Hf because of the larger Lewis acidity of Sn.

Otherwise, both complexes look very similar. The second water molecule can bind in two modes referred to as cis if both water ligands are neighbors, or trans if they are on opposite sides of $M(OH)_4$ (see Figure 3).

The trans isomer shows an unstable behavior in both cases, although different for Hf and Sn. Indeed, no minimum energy was found for Hf, the trans isomer undergoing a barrierless isomerization to the cis form. In the case of Sn, the trans isomer corresponds to an energy minimum, but its value (−35 kJ/mol) is higher than that obtained after the first hydration (−41 kJ/mol). Therefore, this isomer is unstable with respect to the loss of one water ligand. However, an activation barrier is needed for the detachment of this ligand. We believe that this behavior results from the greater flexibility introduced by the presence of Hf low-lying d orbitals. The relative instability of the trans isomers can be ascribed to the fact that the negatively charged OH groups are constrained to remain in a smaller volume than in the cis isomer. For both isomers, the global configurations are very similar. In the case of Sn, this is an octahedron composed of two pyramids having a common square base. However, for the trans isomer (see Figure 3c), the base plane contains the four negatively charged OH groups, showing large electrostatic repulsion. On the other hand, in the cis isomer (see Figure 3b), the base plane contains only three OH groups and one H_2O ligand. The fourth OH group is now out of the plane, reducing electrostatic repulsion.

In the case of the cis isomers, the second water ligand binds by 26 kJ/mol to Hf, which is just slightly lower than the first one (32 kJ/mol), whereas it only binds by 11 kJ/mol to Sn, almost four times less than the first one (41 kJ/mol). The sharp decrease in the binding energies to Sn passing from one to two water ligands is likely to be due to the drop of the Lewis acidity of the tin center after the first complexation, whereas there is an increase of the steric burden with the second water coordination. This phenomenon does not occur for Hf, probably because the Lewis acidity is better conserved upon water complexation, as the d orbitals can take part to the bond, which could explain why the binding energy is better conserved.

Table 3. $M(OH)_4$ Dimerization Energies (energies are given with 2 $M(OH)_4$ as reference)

complex	ΔE (kJ/mol)
$[Hf(OH)_4]_2$ (Figure 4a)	−103
$[Sn(OH)_4]_2$ (Figure 4b)	−91

We also investigated the third hydration of both $M(OH)_4$ precursors. We found that this last ligand is almost not bonded to Hf and not at all to Sn.

The above results show the tendency of metallic element to increase its coordination number, even in the case of a simple precursor molecule. A coordination of up to seven for Hf and up to six for Sn were achieved. However, the last ligand is very weakly bonded in both cases, so we can consider that only the five (Sn) and six (Hf) coordinated complexes are really stable. We can conclude that, for Sn, a more complex system, containing more metallic atoms, is needed to really stabilize the coordination of six, whereas in the case of Hf, six coodination is still far from the maximum coordination, which is eight.

B. Formation of $[M(OH)_4]_2$. To assert this idea, we have investigated more complex systems, performing the dimerization of $Sn(OH)_4$ and $Hf(OH)_4$ without any addition of water molecules. To this end, we approach the two monomers step by step, minimizing the total energy of the system by relaxing all the coordinates but the intermetallic distance. Calculations show that the dimerization reaction occurs with a barrier that is very small (<5 kJ/mol) and whose energy is well below the energy of the reactants ($\Delta E \approx -60$ kJ/mol), meaning that the reaction is barrierless from a practical point of view. The energies are compiled in Table 3.

Looking at the structures in Figure 4, we can see that for both Hf and Sn, the most favorable structure contains 2 OH groups bridging the 2 Hf or Sn atoms leading to pentacoordinated metal centers.

Moreover, there is a noticeable difference between the optimal structures of $[Hf(OH)_4]_2$ and $[Sn(OH)_4]_2$. Although the first one is central symmetric, the second one is planar symmetric, the symmetry plane passing by the bridging O and H atoms. We can see in both $[M(OH)_4]_2$ dimers that two of the hydroxyl groups and the two bridges are almost in the same plane, containing the metal atoms. This can be viewed as a first step toward the cubic HfO_2 and octahedral SnO_2 crystalline structures, because the same symmetries can be found, respectively, in corresponding crystalline oxides.

Another result is that the dimerization energies are larger than the first hydration energies. We can expect that water does not hamper with agregation.

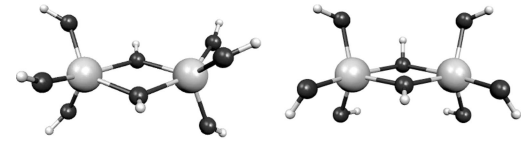

Figure 4. (a) $Hf(OH)_4$ and (b) $Sn(OH)_4$ dimers structures.

Table 4. $M(OH)_4$ Dimer Isomerization and Dehydration Energies (energies are given with $[M(OH)_4]_2$ as reference)

complex	ΔE (kJ/mol)
$(OH)_3Hf-O-Hf(OH)_3(H_2O)$ (Figure 5a)	+41
$(OH)_3Hf-O-Hf(OH)_3$ (Figure 5b) + H_2O	+76
$(OH)_3Sn-O-Sn(OH)_3(H_2O)$ (Figure 5c)	+37
$(OH)_3Sn-O-Sn(OH)_3$ (Figure 5d) + H_2O	+73

This dimerization reaction is remarkable in that it is found to be barrierless, occurring spontaneously wherever two monomers are found close together. However, in the context of ALD, bringing no hydroxylated precursors, one would normally expect to find $(OH)_3M-O-M(OH)_3$ complex, rather than the dimer, because this structure corresponds to the basic element of the oxide. To further investigate this basic assumption, we have calculated the total energies of these structures, isolated and associated with one water molecule, in the two cases of Hf and Sn metallic elements. Results are reported in Table 4.

We can observe that $(OH)_3M-O-M(OH)_3$ complex is less stable, by 76 kJ/mol in the case of Hf and 73 kJ/mol in the case of Sn, with respect to the corresponding dimer complexes. The adsorption of one water molecule on the complex will stabilize it, but we are still at 41 and 37 kJ/mol above the dimer energy for Hf and Sn, respectively. Three conclusions can be drawn from these results. The first is that the tendency to increase the coordination number is stronger than that to cope with the conventional valence of metallic elements. The result is that the dimer configuration is expected to occur frequently on the surface when the bulk coordination number is not yet reached. The dimer configuration should completely disappear deeper in the film, when the bulk coordination number is reached. But the systems investigated in this paper are not sufficiantly large to describe accurately this process. We believe that the transition from the dimer configuration to the $(OH)_3M-O-M(OH)_3$ structure constitutes the essence of the densification mechanism in the ALD process. The second conclusion is the difficulty in removing the water molecule inserted in the films, either in the OH form or as adsorbed molecules. As the third conclusion, it should be noted that the transition from the dimer structure to hydrated $(OH)_3M-O-M(OH)_3$ complex is no more barrierless. This means that the transition needs more energy than the reaction enthalpies of 41 kJ/mol for Hf and 37 kJ/mol for Sn. Again, the effect of larger metal coordination numbers than in the systems under investigation is to lower the activation barriers and the reaction enthalpies.

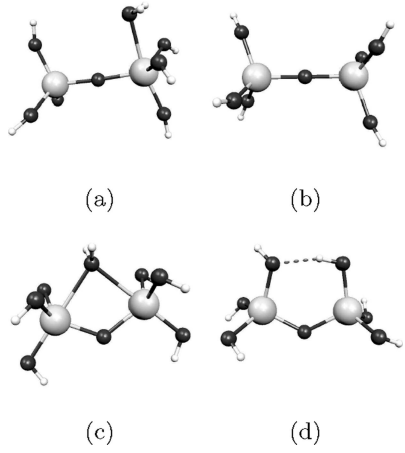

Figure 5. (a) Hydrated and (b) not hydrated $(OH)_3Hf-O-Hf(OH)_3$ and (c) hydrated and (d) not hydrated $(OH)_3Sn-O-Sn(OH)_3$ structures.

Table 5. First and Second $[M(OH)_4]_2$ Hydration Energies[a]

complex	ΔE_{2H_2O}	ΔEH_2O (kJ/mol)
$[Hf(OH)_4]_2(H_2O)$ op (Figure 6a)		−53
$[Hf(OH)_4]_2(H_2O)$ ip (Figure 6b)		−22
$[Sn(OH)_4]_2(H_2O)$ op (Figure 6c)		−30
$[Sn(OH)_4]_2(H_2O)$ ip (Figure 6 (d))		−24
$[Hf(OH)_4(H_2O)]_2$ op (Figure 7a)	−120	−67
$[Hf(OH)_4(H_2O)]_2$ ip (Figure 7b)	−47	−25
$[Sn(OH)_4(H_2O)]_2$ op (Figure 7c)	−104	−74
$[Sn(OH)_4(H_2O)]_2$ ip (Figure 7d)	−51	−24

[a] The op and ip stand for normal and in plane positions of H_2O. For the first hydratation, the energies correspond to the bonding of one water molecule. For the second hydratation, the first column corresponds to the bonding of the two water molecules and the second column to the bonding of the second water molecule on the corresponding (op, ip) monohydrated $(M(OH)_4)_2$.

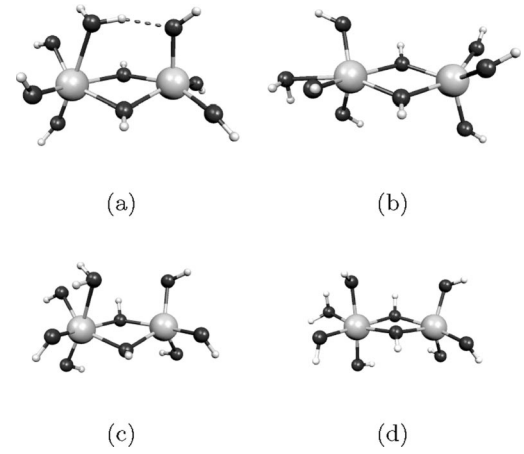

Figure 6. Monohydrated $Hf(OH)_4$ (a) op and (b) ip and $Sn(OH)_4$ (c) op and (d) ip dimers structures.

Finally, calculations show that water desorption from low coordinated systems needs some 45 kJ/mol. Therefore, the water purge during ALD of metallic oxides should therefore be carefully optimized. Also, one should always expect to find water molecules wherever the bulk coordination number is not satisfied in the growing film.

C. Hydration of $[M(OH)_4]_2$. We now try to go further toward the metal oxide structure by hydrating the dimer precursor $[M(OH)_4]_2$. The results of the hydrations energies are given in Table 5.

Two kinds of complexes were considered: one with the two water ligands in the plane made by the bridging OH bonds and metal atoms (which we call ip for "in plane"), the second with the two water molecules perpendicular to this plane making hydrogen bonds with OH (which we call op for "out of plane").

The first and second hydration structures in ip and op configurations are represented in Figures 6 and 7, respectively. The op configuration is shown to be the most favorable for both Hf and Sn, as it allows each water ligand to build hydrogen bonds with an OH group on the other metal center. The energy difference between ip and op configurations ranges from 30 to 70 kJ/mol depending on the metal and the hydration degree. Part of this energy difference

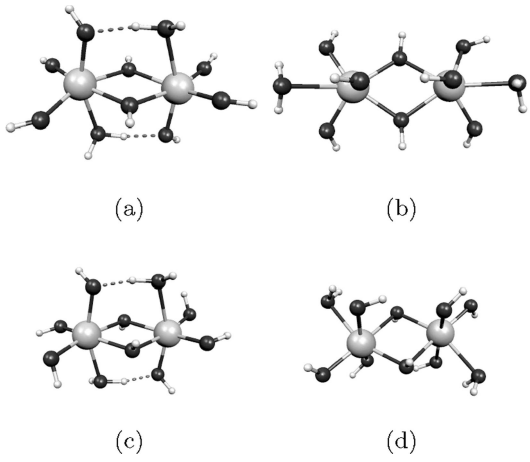

Figure 7. Bihydrated $Hf(OH)_4$ (a) op and (b) ip and $Sn(OH)_4$ (c) op and (d) ip dimers structures.

should be attributed to the formation of hydrogen bonds with the complex, resulting from the nature of the molecules considered, and not necessarily present in the oxide films. Subtracting 25 kJ/mol for each hydrogen bond, the op structures are still more stable than the ip structures. This result is in agreement with the fact that op structures are remarkably close to the bulk oxide structures. Comparing Hf and Sn, we can see again that hydration is more favorable for Hf than for Sn.

D. Application to Film Growth. ALD is the frequently used process for the deposition of high-*k* oxides, and in particular HfO_2, in microelectronics. Although the first aim of this article is not a theoretical investigation of the ALD process, the results presented in the previous sections can be used to improve the film growth process in many respects. Calculations are performed on small size systems not only for computational reasons but mainly to avoid the complexity of the surface structure, in terms of chemical environment and microroughness, during a realistic ALD experiment. Therefore, the results cannot be quantitatively related to an ALD process. Their relevance is rather to bring insights into the process through qualitative agreement. The dimerization/aggregation of hydroxylated metallic precursors certainly shows similar behaviors as the OH terminated species frequently encountered on the substrate surfaces during the ALD process. This is particularly the case near edges or kink sites, where dangling bonds are easily hydroxylated. If the thermodynamic conditions used during the ALD process allow dimerization reactions to occur, they will certainly contribute to the smoothing of the deposited layer. It is clear from the calculations that the tendency of the metallic elements to increase their coordination numbers up to their values in bulk oxides leads these atoms to share their hydroxyl groups, at the price of exceeding their natural chemical valencies. This is very probably the physical origin of the densification mechanism, because it results in the transition from treelike configurations to more compact structures. This mechanism can occur only if the metal precursors are perfectly hydrolyzed after their incorporation on the substrate surface. Chlorine or organic terminals in the precursor molecules, such as $HfCl_4$ or TEMAH (tetra ethyl methyl amide hafnium), can certainly not be shared by two metallic atoms. We can therefore state that the role of water hydrolysis during ALD process is more than just preparing the surface to react with new incoming precursor molecules, as is usually expressed in ALD descriptions. It also consists of sharing hydroxyl groups in view of the further densification of the films. The same reactions will certainly continue to participate in the densification mechanisms and improve the quality of the surface during post-process annealing, if hydroxyl groups are left at the end of the deposition process. The results presented here can also be used for the simulation of film growth by ALD. For example, they show that in simulations based on the kinetic Monte Carlo technique, for example, it is necessary to properly include the hydroxyl sharing mechanisms in the model, with their adequate thermodynamic and kinetic parameters. This type of mechanism is absent in the present simulation packages.

Another point shown by our calculations is the adsorption of water molecules, with relatively large binding energies, to increase the metal coordination wherever the structure of the film does not allow a sufficient coordination. The presence of these water molecules has a non-negligible effect on the further deposition of the oxide, through mechanisms that are not clearly known today. The role of water purge in the ALD process, to completely remove the remaining molecules or remove them partially to take advantage during the subsequent phases of the process, remains an open question.

To answer these questions but also bring quantitative information to the ALD process, we should examine more complex structures. These structures can be guessed from rough kinetic Monte Carlo simulations containing the crude ideas presented here. Our results can therefore be considered as first step of a multiscale modeling strategy, combining ab initio DFT calculations and kinetic Monte Carlo simulations.

Finally, as the results of our calculations, we can observe that OH containing precursors tend to preorganize in the gas phase, giving birth to solidlike aggregates. Obviously, this mechanism cannot happen during a perfect ALD process where all water molecules are purged before the introduction of metallic precursors. But the high probability of occurrence of such barrierless reactions shows that care should be taken to properly design the purge phases. Moreover, if the industrial process has to shift, totally or partially, toward the CVD process, the deposition of aggregated precursors should be considered. These aggregates can lead to the formation of ill-structured metal oxide films. Although this may not be too crucial for the growth of gas sensors SnO_2 films, this is to be avoided for HfO_2 films that will be used in microelectronics.

4. Conclusion

We have performed calculations on the hydration and dimerization of M(OH), with M being Hf or Sn. We have observed that the $M(OH)_4$ precursors have a strong affinity for increasing their coordination number. This increase is done with a rearrangement of the ligands, leading to a more crystalline structure. We have shown that this mechanism

can be observed even with small size molecules, having just one or two metallic atoms. We believe that it will be more pronounced in large size systems, deposited thin films, for example, giving rise to the densification mechanisms. Although the results presented here concern only two types of metallic elements, Hf and Sn, we believe that the tendency is more generic and the above considerations can be usefully applied to other metallic oxides.

Further, our results results show that it is likely that the precursors preorganize in the gaz phase giving rise to solidlike agregates.

Therefore, a particular care should be taken to avoid the presence of any water in the vessel or any OH contamination of the precursors. Such contaminations could lead to cluster deposition regime, because we have shown that dimerization is both favorable and barrierless.

The adsorption of water molecules inside the oxide films to satisfy the lack of coordination of metallic atoms has not been investigated here, but can have a major contribution in ALD process. A series of new mechanisms can be attributed to this effect.

Finally, a multiscale modeling approach to investigate the deposition of high-*k* oxides, mainly based on Hf compounds, is in progress.

Acknowledgment. We thank A.N.R.-05-CIGC-0003-02 LN3M for funding and Groupement Scientifique CALMIP and IDRIS for computational resources. We thank the Conseil Regional de Martinique for its help.

CM071740A